



ORIGINAL ARTICLE

Isolation and identification of bioactive compounds from *Tinospora cordifolia* stem extracts as antibacterial materials in seawater environments



Ahmad Royani^{a,b}, Muhammad Hanafi^{c,d}, Puspa Dewi N. Lotulung^e,
Muhammad Eka Prastya^c, Chandrabhan Verma^f, Azwar Manaf^{a,*},
Akram Alfantazi^f

^a Postgraduate Program of Materials Science Study, Department of Physics, Faculty of Mathematics and Natural Sciences, Universitas Indonesia, Depok 16424, Indonesia

^b Research Center for Metallurgy, National Research and Innovation Agency – BRIN, Kawasan Puspiptek, Tangerang Selatan 15314, Indonesia

^c Research Center for Pharmaceutical Ingredients and Traditional Medicine, National Research and Innovation Agency – BRIN, Kawasan Puspiptek, Tangerang Selatan 15314, Indonesia

^d Faculty of Pharmacy, Pancasila University, Jakarta Selatan 12640, Indonesia

^e Research Center for Chemistry, National Research and Innovation Agency - BRIN, Kawasan Puspiptek, Tangerang Selatan 15314, Indonesia

^f Department of Chemical Engineering, Khalifa University of Science and Technology, P.O. Box 127788, Abu Dhabi, United Arab Emirates

Received 31 January 2023; accepted 15 May 2023

Available online 19 May 2023

KEYWORDS

Antibacterial;
Bioactive material;
Isolation;
N-trans-Feruloyltyramine;
P. aeruginosa;
Tinospora cordifolia

Abstract The *Tinospora* genus is widely utilized because of its numerous bioactive compounds. This work aimed to isolate the bioactive constituents and antibacterial activities of the *T. cordifolia* plant. Maceration, column chromatography, and thin-layer chromatography plates were utilized to identify and visualize the extracted and isolated compounds. Total phenolics and flavonoids in the extracts and active fractions were also analysed. Substances were identified through their molecular structure and molecular mass. The names, molecular weights, and structures of the components of the test materials were verified using Fourier transform infrared (FT-IR) spectroscopy and nuclear magnetic resonance (¹H NMR, ¹³C NMR, HMQC, and HMBC). The minimum inhibitory concen-

* Corresponding author at: Postgraduate Program of Materials Science Study, Department of Physics, Faculty of Mathematics and Natural Sciences, Universitas Indonesia, Depok 16424, Indonesia.

E-mail addresses: ahmad.royani@brin.go.id (A. Royani), azwar@sci.ui.ac.id (A. Manaf), akram.alfantazi@ku.ac.ae (A. Alfantazi).

Peer review under responsibility of King Saud University.



tration (MIC) values were 3294, 156, and 32 $\mu\text{g/mL}$ for the crude extract, active fraction, and isolate of *T. cordifolia*, respectively. The total phenol active fraction was 38.44 mg GAE/g, while the total flavonoid content was 79.46 mg QE/g. *N-trans-Feruloyltyramine* or Moupinamide, a phenol group compound with a molecular ion weight of 314 m/z ($M + H$)⁺, was successfully isolated as the bioactive compound. The moupinamide isolate may be responsible for the antibacterial activity of *T. cordifolia* in this work. Our findings indicate that the bioactive isolate from *T. cordifolia* is a potential source of green material and exhibits the potential to inhibit *P. aeruginosa* biofilm, which is responsible for microbial corrosion.

© 2023 The Author(s). Published by Elsevier B.V. on behalf of King Saud University. This is an open access article under the CC BY-NC-ND license (<http://creativecommons.org/licenses/by-nc-nd/4.0/>).

1. Introduction

Microbiologically influenced corrosion is a type of corrosion that is induced or accelerated by specific microorganisms or metabolic products (Marciales et al., 2019). *Pseudomonas aeruginosa* is a Gram-negative facultative aerobic bacterium that produces biofilms on metal surfaces and promotes corrosion (Jia et al., 2017; Cardona and Muñoz Mata, 2013). *P. aeruginosa* causes corrosion in the marine environment by forming biofilms (Pu et al., 2020; Lekbach et al., 2018). The corrosion mediated by *P. aeruginosa* has been shown to decrease the performance of pipe network systems that distribute water (Lekbach et al., 2018). It is critical to use inhibitors to control corrosion and prevent material damage caused by corrosion (Nikitasari et al., 2020). Many synthetic compounds are highly resistant to corrosion, but most are highly toxic to the environment (Verma et al., 2018). Because of the growing awareness of green chemistry and sustainable development, using chemicals derived from plants is becoming increasingly popular in many industrial applications, such as corrosion inhibition. Due to their affordability, availability, renewability, ecological acceptability, and ecologically friendly qualities, green inhibitors or green biocides from plants have recently undergone tremendous growth and advancements (Royani, Hanafi and Manaf, 2022; Satheesh et al., 2016). On the other hand, due to the large variety of bioactive molecules that plants produce, they are a potential source of antibacterial agents against *P. aeruginosa* (Parthipan et al., 2018; Swaroop et al., 2016; Parthipan et al., 2021). In order to create and exploit bioactive components that are more efficient at resolving corrosion issues brought on by the *P. aeruginosa* biofilm bacterium, researchers can benefit from harvesting and separating bioactive compounds.

Tinospora cordifolia is a tropical vine belonging to the Menispermaceae family utilized as a traditional medicinal herb. Due to its bioactive compounds, *T. cordifolia* has been widely studied in literature from various scientific disciplines. Various extracts, fractions, and constituents were examined and several bioactive substances were quantitatively evaluated (Singh and Chaudhuri, 2017). According to previous studies, the dominant phytochemical elements of the genus *Tinospora* are quaternary alkaloids (Yusoff et al., 2014). The other results indicated that the extract of *T. cordifolia* included pharmacologically active chemicals that exhibit potent antioxidant and antibacterial properties (Ramesh et al., 2016). Another study stated that crude extracts and isolated chemicals from *T. crispa* possess different pharmacological properties, such as antioxidant, anti-inflammatory, cytotoxic, and antidiabetic properties (Ahmad et al., 2016). Although there have been numerous studies on the extraction and use of *T. cordifolia* in medicine and pharmaceuticals, to the best of our knowledge, no research has isolated bioactive components from this species to create corrosion biofilms through green antibacterial material. In this case, further research is needed to explore this type of plant because of its extraordinary potential to inhibit and control various microbes.

Previous studies on crude extract have demonstrated that *T. cordifolia* stem extract exhibits antibacterial activity against *P. aeruginosa* (Royani et al., 2023), inspiring more investigation into these positive qualities of the plant and possible applications. This

work focused on isolating and assessing the antibacterial activity of the identified bioactive compounds due to their promising biological properties. This work aimed to identify bioactive chemicals as sustainable materials for growing antibacterial biofilms in synthetic seawater media. *T. cordifolia* was utilized in this investigation because it is a medicinal herb that contains numerous bioactive components. Extracts and isolation were performed using maceration, column chromatography, and thin-layer chromatography. The antibacterial activity against *P. aeruginosa* was assessed by dilution in synthetic seawater broth. Utilizing AlCl_3 and Folin-Ciocalteu calorimetry, the flavonoid and phenolic contents were evaluated. Pure isolates/compounds were distinguished by FT-IR, ¹H NMR, ¹³C NMR, HMQC, and HMBC.

2. Materials and methods

2.1. Materials

Tinospora cordifolia plants were provided by the Indonesian Medical and Aromatic Crops Research Institute (IMACRI) - Bogor. The plant samples were identified in the Herbarium Bogoriense laboratory, Directorate of Scientific Collection Management of BRIN, Cibinong – Bogor (ID number: B-18 10/II.6.2/DI.05.07/6/2022). *Pseudomonas aeruginosa* (ATCC 15,442 strain) was obtained from IPB University Culture Collection (IPBCC) – Department of Biology, IPB University.

The solvents for extraction, fractionation, and isolation were distilled methanol, n-hexane, ethyl acetate, and distilled water. TLC silica gel sheet 60 F₂₅₄ aluminium sheets (Merck, 1.05554.0001) were used for thin layer chromatography, and silica gel (0.063–0.200 mm, Merck 1.07734.1000) was used for column chromatography. The antibacterial test materials were Brain Heart Infusion (BHI, BD, Bacto 237500), Mueller Hinton Agar (MHA), and synthetic seawater media (Marine Art, SF-1, Japan). Both tetracycline and ampicillin (Sigma) were used for positive control.

2.2. Extract preparation

The stems of *T. cordifolia* plants were washed and dried before being cut into small pieces and pulverized in a blender. The powdered simplicia was stored in a closed container at room temperature. One thousand grams of powdered simplicia were extracted using the repeated maceration method with 50% methanol (v/v) in the macerator for three consecutive days. The filtrate was filtered and evaporated using a rotary vacuum evaporator after maceration. Furthermore, the extract was collected, weighed, and refrigerated until further processing.

2.3. Isolation of the active compounds

The flow chart in Fig. 1 shows the process of isolating the active compound from the *T. cordifolia* plant extract. The extract was fractionated using column chromatography and solvents containing n-hexane, ethyl acetate, and methanol. After preparation, 12.5 g of crude stem extract was slowly added to the column. In this study, column chromatography used a flow rate of 2 mL/min with 100 mg/mL of concentration and 125 mL of volume. After that, the eluent was streamed and collected. The eluent was gradually changed from nonpolar to polar. A rotary vacuum evaporator was used to collect and evaporate the results of the column chromatographic elution. The fraction concentrates were then visualized, and aggregation was performed using the same thin-layer chromatography (TLC) profile. The active fraction was then isolated using a two-stage column chromatography method. 94.5 mg of the active fraction was prepared with a volatile solvent, 90 mg of silica gel was added, and the mixture was loaded into the chromatography column. The column chromatography elution results were placed in a vial and dried in an oven. The isolates or subfractions were then separated using TLC to produce pure isolates and combinations based on the same TLC profile. The subfraction (isolate) was weighed and placed in a bottle, and its activity was determined. Furthermore, for pure isolates, the compound structure was analysed and identified.

2.4. Phenolic and flavonoid content analyses

The total phenolic content (TPC) of the resulting extract and active fraction was analysed using the Folin-Ciocalteu method (Singleton, Orthofer, and Lamuela-Raventós, 1999) with gallic acid as a standard. Pipette 500 L of sample solution and reference solution (25, 50, 100, 150, and 200 μ L) into a test tube and dilute with 250 μ L of Folin-Ciocalteu reagent and distilled water to a volume of 4 mL. After 8 min, 750 μ L of 20% Na_2CO_3 was added and shaken until homogeneous. The mixing solution remained at room temperature for 2 h. Absorption was measured at a wavelength of 765 nm. Each measurement was repeated twice to obtain the average phenol content. The total phenolic content was represented as gallic acid equivalents (mg/g extract) by using the calibration regression equation of the curve.

Meanwhile, the total flavonoid content was analysed by the colorimetry aluminium chloride (AlCl_3) method described by Chang et al. with slight modification (Chang et al., 2002). 4 mg of quercetin was dissolved in 4 mL methanol. The standard curve measurements used 10, 20, 30, 40, and 50 μ g/mL concentrations with standard solution volumes of 50, 100, 150, 200, and 250 μ L. Each test tube (standard and sample) received 2 mL of distilled water and 150 μ L of NaNO_2 (5%). After 5 min, 150 μ L of AlCl_3 (10%) was added. After 6 min, 2 mL of 1 M NaOH was added, and the volume was adjusted

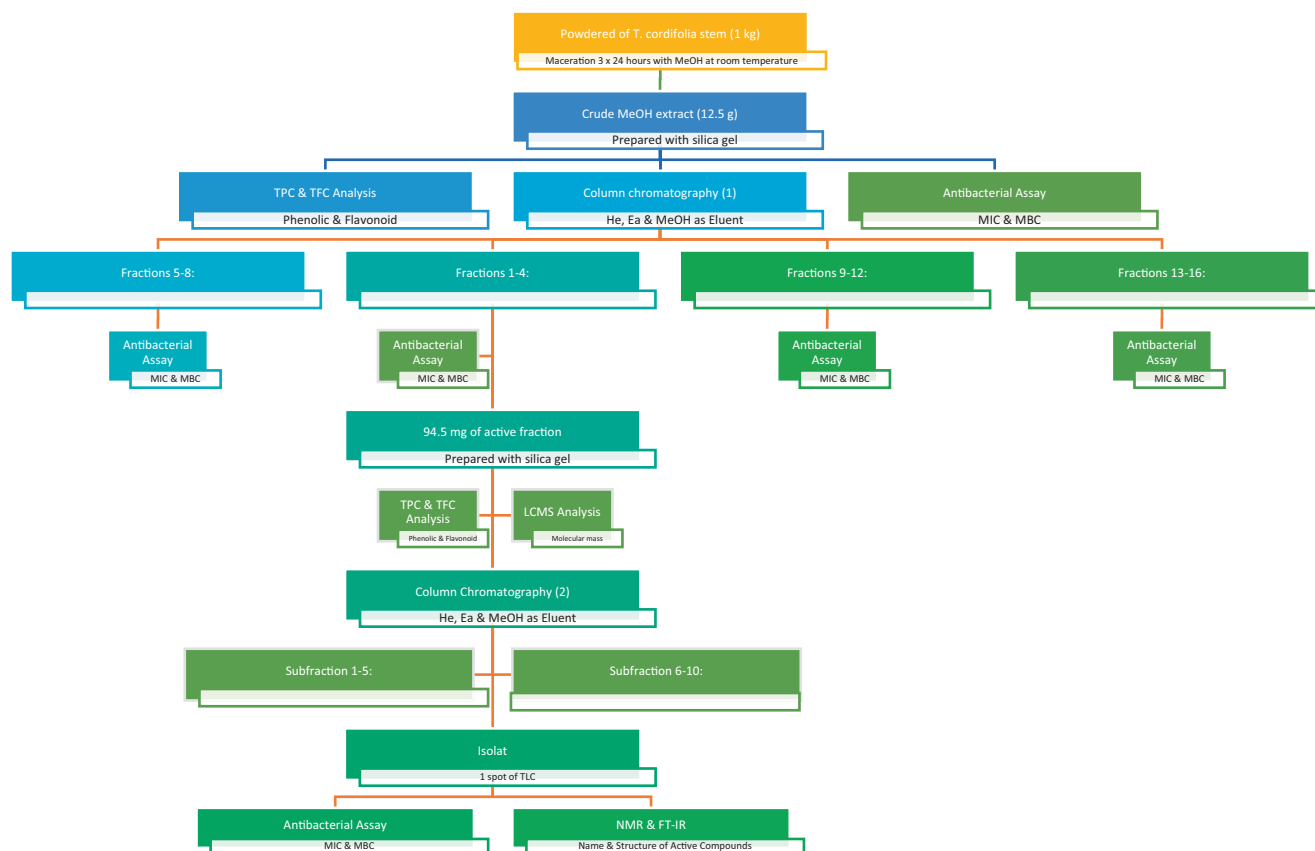


Fig. 1 Flowchart of the isolation of bioactive compounds from *T. cordifolia* plants consisting of crude extract maceration, including initial column chromatography, secondary column chromatography with the most active fraction, and identification of the isolated compounds.

with distilled water to 5 mL. After homogenizing the solution mixture, the absorbance was measured using a UV-Vis spectrophotometer at 510 nm.

2.5. Antibacterial assay

Antibacterial activity was assessed by serial broth dilution methods following previous methods as described elsewhere (Priyanto et al., 2022). Before the antibacterial test, all instruments were cleaned and sterilized in a UV chamber for 24 h. The media and nutrients were prepared according to the manufacturer's instructions and autoclaved for 15 min at 121 °C. The 96-well microplate well (Iwaki) was filled with 100 µL of BHI medium (diluted with artificial seawater), and well (A) was filled with 100 µL of the extract solution (diluted on methanol) before generating a series of dilution concentrations (serially dilution was set starting from 5000 to 50 µg/mL for fraction samples, and from 300 to 10 µg/mL for sub-fraction and isolate samples). Next, 100 µL of the 24-hour cultured bacterial suspension was added to each well plate and incubated at room temperature for 24 h. This study used the standard McFarland 0.5 of 24-hour bacterial culture, equivalent to 1×10^8 CFU/mL. The turbidity and clarity of each incubated test medium were compared to the control media solution to determine the minimum inhibitory concentration (MIC). When the inhibition of bacterial growth is at a lower concentration, referred to as the MIC value, the test (Mueller Hinton Agar (MHA) media is clearer. After incubation, the minimum bacterial concentration (MBC) was observed by searching for areas on the agar medium with no bacterial growth.

2.6. Analysis thin layer chromatography (TLC)

TLC analysis isolated or separated the active compound from the liquid solution. Aluminium plates and silica gel 60 F₂₅₄ as the stationary phase were used for TLC analysis. The mobile phase (eluent) was a mixture of n-hexane, ethyl acetate, and methanol. The sample (fraction/isolate) was dissolved in the appropriate solvent and shaken until completely dissolved. Furthermore, the solution was spotted on the bottom plate line (1 cm from the bottom), dried, and then eluted in a chamber containing eluent in a specific ratio. The plates were removed and dried after being completely adsorbed (up to the top line of the plates). The spots formed were observed at wavelengths of 254 and 366 nm.

2.7. Identification of bioactive compounds by LC-MS, FT-NMR, and FT-IR

The molecular weights of the compounds were determined using liquid chromatography-mass spectrometry (LC-MS) with a UNIFI chromatography instrument (Xevo G2-XS QToF) equipped with Mariner Biospectrometry software. The LCMS test was performed with methanol solvent, a 5 µL injection volume, and a C-18 column (15 mm × 2 mm) with a 0.2 mL/minute flow rate. Furthermore, Fourier transfer nuclear magnetic resonance (FT-NMR) JEOL JNM 500 MHz was used to identify pure compounds from isolated results, such as proton (¹H NMR), carbon (¹³C NMR), and 2D-NMR, which included HMQC and HMBC. Approximately 3 mg of the pure isolate was dissolved in a special deuterated

solvent (CD₃OD) and then placed in a unique glass tube for NMR in the centre of the magnetic field tank to be measured by NMR. The functional groups (chemical bonds) of the compounds were detected using Fourier transform infrared spectrometry (FT-IR) (Bruker-Tension II). The scan frequency range was 4000 cm⁻¹ to 500 cm⁻¹, with a resolution of 4 cm⁻¹ for 45 s.

3. Results and discussion

3.1. Yield extract

In this study, the maceration technique was used to obtain yield extracts because, compared to other techniques, maceration is a more straightforward process, requires less equipment and is widely used on a large scale (Vongsak et al., 2013). *T. cordifolia* stem extract with 50% methanol solvent yielded a 20.35% yield. This study calculated yield by weighing the dry extract (concentrated extract) and dividing it by the initial weight (powdered plant material). The extraction efficiency is influenced by extraction time, temperature, method, solvent, and phytochemical composition (Elboughdiri, 2018; Ida Madiha et al., 2017). Because methanol has a boiling point of 65 °C, it is commonly used as a solvent in maceration. In comparison, ethanol has a boiling point of 78 °C, and ethyl acetate has a boiling point of 77.1 °C (Nawaz et al., 2020). As a result, the temperature used to evaporate the resulting extract with methanol solvent is not too high, reducing the risk of overheating and destroying the secondary metabolite content of the extract. As a result, the time needed to evaporate the sample is relatively short.

3.2. Fractionation and antibacterial activity

Fractionation was accomplished through column chromatography with silica gel as the stationary phase and combined solution as the mobile phase. The mobile phases in the fractionation mixtures were hexane, ethyl acetate, and methanol solvents with increasing polarity. Table 1 shows the *T. cordifo-*

Table 1 *T. cordifolia* stem extract fractionation results with several ratios of the eluent.

Component	Eluent	Weight (mg)	Yield (%)
Fraction 1	n-Hex: AcOEt (3:1)	82.2	0.66
Fraction 2	n-Hex: AcOEt (2:1)	121.1	0.97
Fraction 3	n-Hex: AcOEt (1:1)	177.4	1.42
Fraction 4	n-Hex: AcOEt (1:1)	288	2.30
Fraction 5	n-Hex: AcOEt (1:2)	149.4	1.20
Fraction 6	n-Hex: AcOEt (1:2)	628.9	5.03
Fraction 7	n-Hex: AcOEt (1:2)	79.6	0.64
Fraction 8	n-Hex: AcOEt (0:1)	1300.4	10.40
Fraction 9	n-Hex: AcOEt (0:1)	336.9	2.70
Fraction 10	n-Hex: AcOEt (0:1)	16.1	0.13
Fraction 11	AcOEt: MeOH (9:1)	319.3	2.55
Fraction 12	AcOEt: MeOH (8:2)	243.3	1.95
Fraction 13	AcOEt: MeOH (8:2)	532.9	4.26
Fraction 14	AcOEt: MeOH (7:3)	471	3.77
Fraction 15	AcOEt: MeOH (1:1)	957.5	7.66
Fraction 16	AcOEt: MeOH (0:1)	2742.9	21.94

lia stem extract fractionation results and the eluent ratio after combining based on similarities in TLC spots. Methanol produced the highest yield (21.94%), followed by ethyl acetate (10.40%). The type, composition, and activities of the extracted phytochemicals were influenced by the polarity of the solvent used in extraction and fractionation (Nawaz et al., 2020). Ethyl acetate is a semipolar solvent (index polarity of 4.4) that can dissolve alkaloids, flavonoids, sterols, and terpenoids. Methanol is polar (with an index polarity of 5.1). It can dissolve polar compounds, such as amino acids, flavones, flavonoids, glycosides, polyphenols, saponins, phenolic compounds, tannins, and terpenoids (Sri Widyawati et al., 2014). Furthermore, hexane is nonpolar but can dissolve lignin, lipids, terpenoids, and sterols (Sri Widyawati et al., 2014). This result demonstrates that *T. cordifolia* contains more phytochemicals with polar properties.

Additionally, the flow velocity influences the fractionation process, which is affected by gravity, the polarity of the eluent, and the density of the stationary phase (silica gel) (Ravisankar et al., 2019; Pirrung et al., 2018). In addition, the resulting fractions were subjected to an antibacterial test to determine their antibacterial activity level and the fraction's minimal inhibitory concentration. Table 2 displays the antibacterial activity of *T. cordifolia* stem extract fractions against *P. aeruginosa* bacteria. According to the antibacterial activity results, the 1st and 2nd fractions exhibited the lowest minimum inhibitory concentration (MIC) values (140 and 156 µg/mL). In contrast, the minimum inhibitory concentration (MIC) of positive control (tetracycline and ampicillin) was 3.9 µg/mL. The MIC values of the 1st and 2nd fractions are close to those of the positive control, indicating that the 1st and 2nd fractions possess a potent inhibitory effect; consequently, they were isolated for the subsequent processes.

Table 2 Results of the antibacterial activity against *P. aeruginosa* from various fractions.

Component	Concentration (µg/mL)	
	MIC	MBC
Crude extract	3293.75	> 6587.5
Fraction 1	140.625	> 128.25
Fraction 2	156.25	> 312.5
Fraction 3	284.375	> 568.75
Fraction 4	1325	2650
Fraction 5	1500	3000
Fraction 6	3562.5	7125
Fraction 7	1312.5	2625
Fraction 8	1868.75	3737.5
Fraction 9	1762.5	> 3525
Fraction 10	1006.25	> 2012.5
Fraction 11	3387.5	6775
Fraction 12	1125	> 2250
Fraction 13	2875	5750
Fraction 14	4437.5	8875
Fraction 15	2850	5700
Fraction 16	4825	9650
Positive control (tetracyclin)	3.9	7.8
Positive control (ampicillin)	3.9	7.8
Negative control (methanol)	–	–

3.3. Total phenolic and flavonoid contents

The Folin-Ciocalteu and colorimetric aluminium chloride (AlCl₃) methods were used to determine the increase in the content of these two phytochemicals (phenolic and flavonoids) in the active fraction. The TPC and TFC values of the initial extract increased significantly, according to the results in Table 3.

The total phenolic content and bioactive properties of extracts significantly impact their antioxidant and antimicrobial activities (Sukiman et al., 2022). Studies have shown that an increase in the phenolic content of plant extracts leads to an increase in antioxidant and antibacterial activity (Kadir, 2021). Correlation studies of phytochemical content on biological activity were also conducted in the *T. crispera* stem extracts (Sukiman et al., 2022). Based on the TPC and TFC values, it is highly probable that the active fraction belongs to the phenol group and is responsible for antibacterial activities. Therefore, isolation and further analysis are needed to obtain the active compound and its molecular structure.

3.4. LCMS of active fractions

The analysis result of liquid chromatography-mass spectrophotometry (LCMS) for the active fraction is presented in Fig. 2.

The active fraction chromatogram results are shown in Fig. 2, and there is a peak with a high intensity at a retention time of 1.9 min. At 1.9 min of retention time, a dominant (high) spectrum, m/z 314.22 (M + H)⁺, indicates a molecular weight of 313.22. Previous researchers reported that the m/z spectrum of 312.1235 (M–H)⁺ indicated the compound *N-trans*-feruloyltyramine (Khan et al., 2021). Another study found an *N*-feruloyl tyramine compound in the 314 (M + H)⁺ spectrum (Sun et al., 2019). These findings support previous findings that the *T. cordifolia* plant contains the compound *N-trans*-feruloyltyramine, also known as moupinamide, with a molecular weight of 313.13141 (Royani et al., 2023).

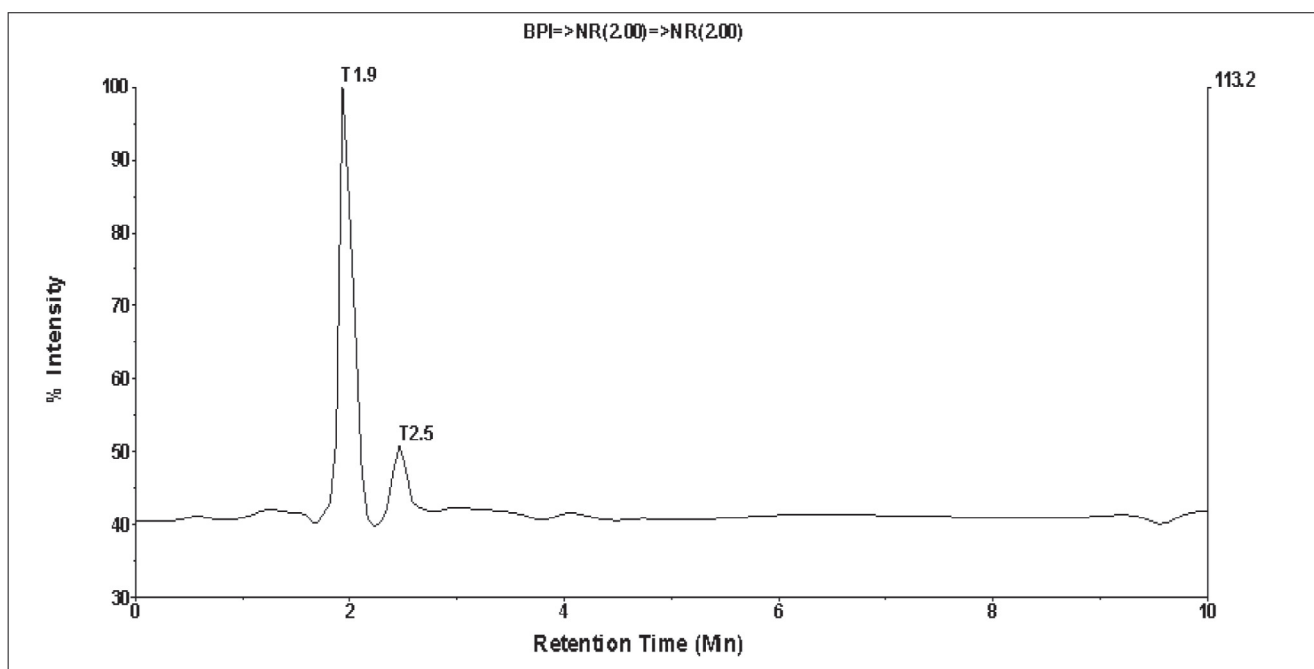
3.5. Isolation of the active Fraction and antibacterial properties

The active fraction was isolated to obtain pure isolates with activity against *P. aeruginosa* bacteria. Table 4 shows the mass gain results and the eluent ratio used.

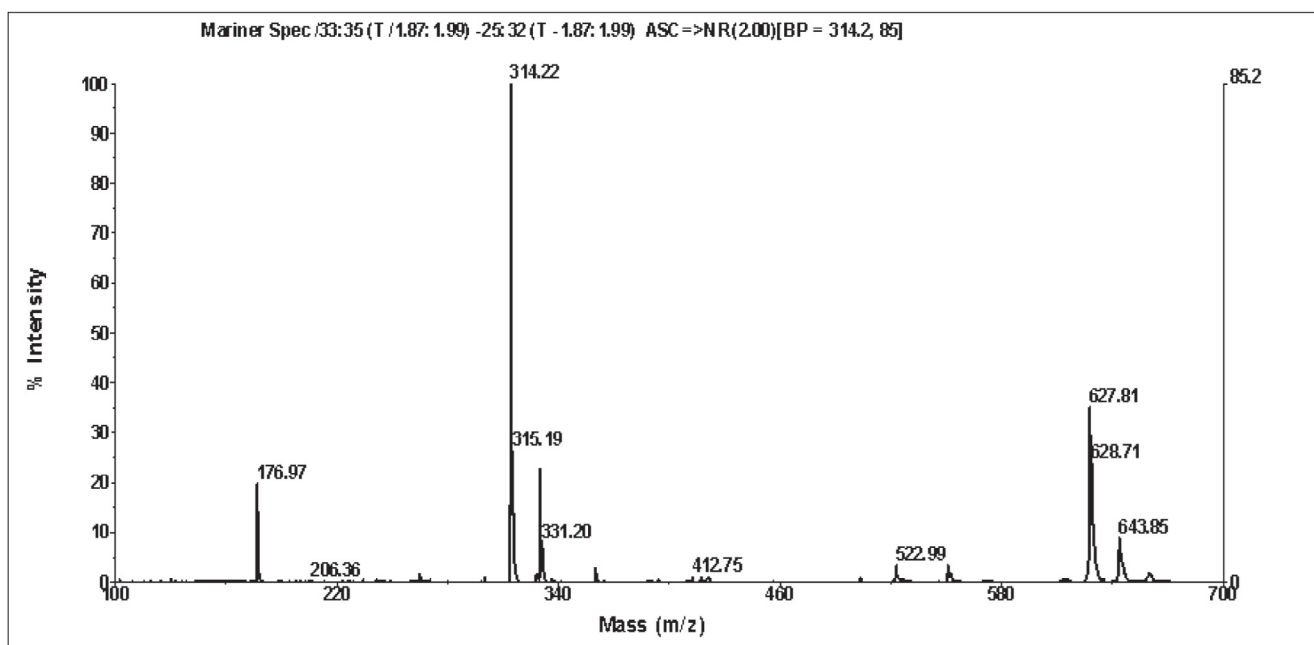
Based on the similarity of the TLC plate results, ten sub-fractions were obtained from the isolation process. The fifth subfraction showed the highest mass gain (40.2 mg) of approximately 42.5%. The 7th fraction exhibited the lowest mass gain (about 3 mg) and is indicated as a pure compound with a single TLC spot, as shown in Fig. 3.

Table 3 Comparison of TPC and TFC values in crude extracts and active fractions from *T. cordifolia* plants.

Component	TPC (GAE/g, %)	TFC (QE/g, %)
Crude extracts (50% methanol)	6.56 ± 0.17	0.33 ± 0.04
Active fraction	38.44 ± 0.24	79.46 ± 1.00



(a). Chromatogram of the active fractions.



(b). Mass spectrum at a retention time of 1.9 minutes.

Fig. 2 Results of LCMS analysis for active fractions.

The subfractions were then subjected to antibacterial tests to determine their activity against bacterial inhibition. [Table 5](#) summarizes the findings of the antibacterial activity test performed on each subfraction against bacteria capable of forming biofilms.

The results of the antibacterial activity revealed that the minimum inhibitory concentration (MIC) values ranged from 16 to 128 $\mu\text{g}/\text{mL}$ with varying minimum bacterial con-

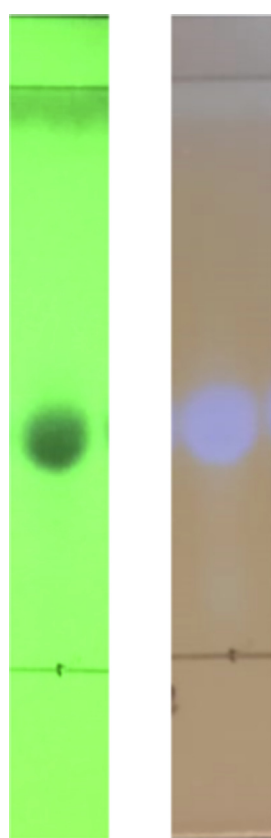
centration (MBC) values, as shown in [Table 5](#). Antibacterial activity from the subfraction results tended to be much stronger than that of the fractions and extracts, which could occur because the secondary metabolite content in the subfraction was purer, which significantly impacted its activity. In addition to the bacterial test, pure isolates were analysed with FT-IR, ^1H NMR, and ^{13}C NMR to determine their molecular structure.

Table 4 Results of subfraction, mass, and eluent from the active fraction of *T. cordifolia* stem extracts.

Component	Eluent	Weight (mg)	Yield (%)
Sub-Fraction 1	n-Hex: AcOEt (3:1)	6	6.35
Sub-Fraction 2	n-Hex: AcOEt (2:1)	5.5	5.82
Sub-Fraction 3	n-Hex: AcOEt (1:1)	4.7	4.97
Sub-Fraction 4	n-Hex: AcOEt (1:2)	5.2	5.50
Sub-Fraction 5	n-Hex: AcOEt (0:1)	40.2	42.54
Sub-Fraction 6	AcOEt: MeOH (9:1)	6.4	6.77
Sub-Fraction 7	AcOEt: MeOH (8:2)	3	3.17
Sub-Fraction 8	AcOEt: MeOH (7:3)	3.6	3.81
Sub-Fraction 9	AcOEt: MeOH (1:3)	3.2	3.39
Sub-Fraction 10	AcOEt: MeOH (0:1)	14.3	15.13

Table 5 Results of MIC and MBC of subfraction against *P. aeruginosa* in synthetic seawater media.

Component	Concentration ($\mu\text{g/mL}$)	
	MIC	MBC
Sub-Fraction 1	64	> 128
Sub-Fraction 2	64	> 128
Sub-Fraction 3	32	> 64
Sub-Fraction 4	16	> 32
Sub-Fraction 5	64	> 128
Sub-Fraction 6	128	> 256
Sub-Fraction 7	32	> 64
Sub-Fraction 8	32	> 64
Sub-Fraction 9	42.5	> 85
Sub-Fraction 10	Not detected	Not detected
Positive control (tetracyclin)	3.9	7.8
Negative control (methanol)	–	–

**Fig. 3** Spot TLC isolate results under UV lamp 254 and 366 nm of *T. cordifolia* subfraction 7th.

3.6. Identification of bioactive compounds

The ^1H NMR and ^{13}C NMR spectra of the pure isolate are shown in Fig. 4 and Table 6, respectively. The results of the ^1H NMR spectrum of the isolate indicate that there are two aromatic rings, namely, the substitution at 1–4 (A2B2) on the benzene ring, in which the two signals overlap because they are symmetrical, namely, at δ_{H} 6.72 (2H, d, 8 Hz) and δ_{H} 7.06 (2H, d, 8 Hz). The aromatic ring with the ABX system (trisubstituted at C 1, 3, and 4) at δ_{H} 6.79 (d, 8 Hz), 7.01 (dd, 1.5;

8 Hz), and 7.15 (d, 1.5 Hz). Trans double bonds were detected at δ_{H} 6.40 (d, 16 Hz) and 7.42 (d, 16 Hz), and $\text{CH}_2\text{-CH}_2$ groups were detected at δ_{H} 2.75 (2H, t, 7 Hz) and 3.47 (2H, t, 7 Hz). In addition to a methoxy group ($-\text{OCH}_3$) at 3.87 (s), as summarized in the structure shown in Fig. 4. The ^1H NMR and ^{13}C NMR (Table 6) spectral data are consistent with published data (Al-Taweel et al., 2012; Jiang et al., 2015; Marques et al., 2022).

According to the specific results of ^1H NMR and ^{13}C NMR spectral data, this isolate was identified as N-(4-hydroxy-3-methoxy-E-cinnamoyl)-4-(2-aminoethyl) phenol, the synonym of which is 4-(2-aminoethyl) N-trans-feruloyltyramine and moupinamide, with the structure shown in Fig. 4. This compound has never been reported in *T. cordifolia* previously. However, N-trans-Feruloyltyramine has been isolated from other species, including *Smilax aristolochifolia* (Amaro et al., 2014), *Polyalthia suberosa* (Soi-ampornkul et al., 2022), *Solanum procumbens* (Solanaceae) (Tran et al., 2019), *Datura metel* (Xu et al., 2018), and *Bassia indica* (Othman et al., 2021). This assumption was supported by the results of the ^{13}C NMR spectrum measurements (Table 6) and the H and C correlation measurements (HMQC), as shown in Fig. 4 and Table 6.

Then, as shown in Fig. 5, the results are supported by HMBC long-range correlation, which can determine the position of the chemical movement value in the molecular structure. The primary correlation of HMBC also reveals two aromatic rings on the benzene ring (at δ_{H} 6.72 (2H, d, 8 Hz) and 7.06 (2H, d, 8 Hz)) as well as aromatic rings at δ_{H} 6.79 (d, 8 Hz), 7.01 (dd, 1.5; 8 Hz), and 7.15 (dd, 1.5; 8 Hz) (d, 1.5 Hz). Furthermore, trans double bonds were discovered at δ_{H} 6.49 (d, 16 Hz) and 7.42 (d, 16 Hz), as well as the presence of $\text{CH}_2\text{-CH}_2$ groups at δ_{H} 2.75 (2H, t, 7 Hz) and 3.47 (d, 16 Hz) (2H, t, 7 Hz). The long-range correlation coupling in the HMBC spectrum between the signal (3H, 3.87, s) and C at 149.94 can be used to determine the position of the methoxy group at C-3.

Fig. 6 shows the FT-IR spectrum of the *T. cordifolia* isolates, which confirms the presence of the Moupinamide compound. Significant absorption bands at $3350\text{--}3300\text{ cm}^{-1}$ (N–H bending) and 1651 cm^{-1} (C=O stretch) in the IR spectra of the isolate indicate the amide function. An aromatic

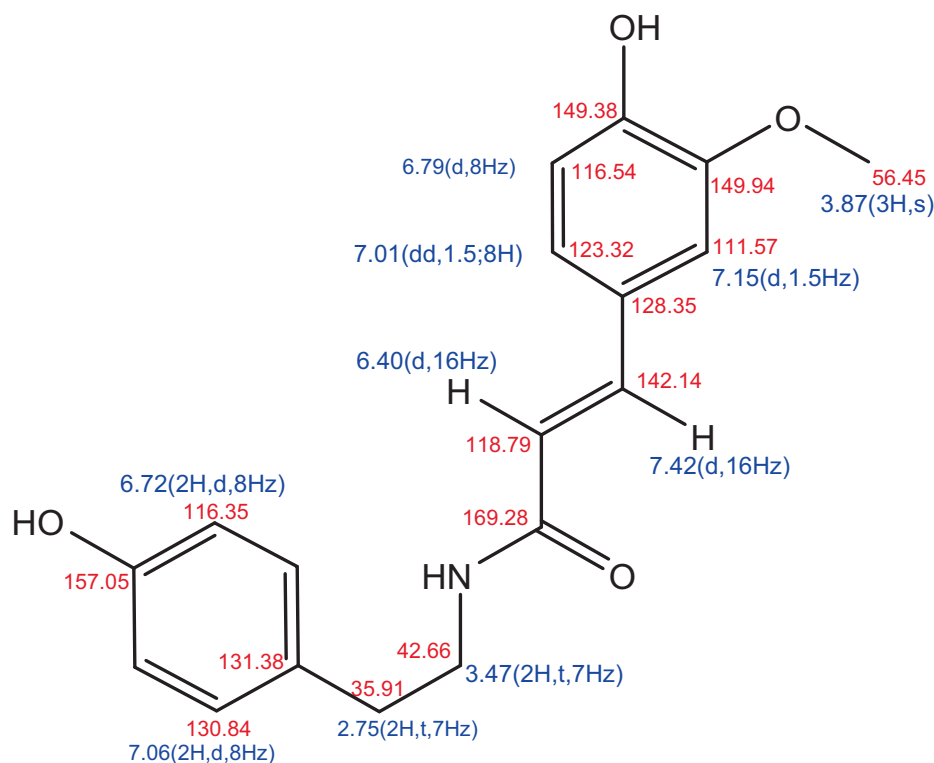


Fig. 4 Analysis of isolated bioactive compounds (N-(4-hydroxy-3-methoxy-E-cinnamoyl)-4-(2-aminoethyl) phenol) with HMQC.

Table 6 Tabulation of chemical shift data from ^1H NMR and ^{13}C NMR spectra of bioactive isolates versus references.

Position		Isolate in this study (500 MHz in CD_3OD)		Reference (Al-Taweel et al., 2012) (500 MHz in CD_3OD)		Reference (Jiang et al., 2015) (150 and 600 MHz in CD_3OD)		Reference (Marques et al., 2022) (50 and 200 MHz in CD_3OD)	
		$\delta^{13}\text{C}$	$\delta^1\text{H}$	$\delta^{13}\text{C}$	$\delta^1\text{H}$	$\delta^{13}\text{C}$	$\delta^1\text{H}$	$\delta^{13}\text{C}$	$\delta^1\text{H}$
1	C	128.35		128.2		128.5		128.22	
2	CH	111.57	7.15 (d, 1.5 Hz)	111.5	7.13 (d, 1H, 1.2 Hz)	111.8	7.12 (1H, d, 1.8 Hz)	111.45	7.04 (brd, 1H, 8 Hz)
3	C	149.94		149.3		149.5		149.87	
4	C	149.38		149.8		150.0		149.22	
5	CH	116.54	6.79 (d, 8 Hz)	116.4	6.81 (d, 1H, 8.5 Hz)	116.7	6.81 (1H, d, 8.4 Hz)	116.43	6.79 (d, 1H, 8 Hz)
6	CH	123.32	7.01 (dd, 1.5; 8 Hz)	123.2	7.048 (dd, 1.2; 8.5 Hz)	123.4	7.03 (1H, dd, 1.8 Hz)	123.21	7.03 (bs, 1H)
7	CH	142.14	7.42 (d, 16 Hz)	142.0	7.44 (d, 1H, 15.5 Hz)	142.4	7.46 (1H, d, 15.6 Hz)	142.02	7.43 (d, 15.8 Hz)
8	CH	118.79	6.40 (d, 16 Hz)	118.7	6.41 (d, 1H, 15.5 Hz)	118.9	6.42 (1H, d, 15.6 Hz)	118.69	6.4 (d, 1H, 15.8 Hz)
9	C	169.28		169.2		169.4		169.15	
1'	C	131.38		131.3		131.5		131.26	
2', 6'	2 CH	130.84	7.06 (2H, d, 8 Hz)	130.7	7.07 (d, 2H, 8.4 Hz)	131.0	7.06 (2H, dd, 2.4 Hz)	130.73	7.10 (2H, d, 8 Hz)
3', 5'	2 CH	116.35	6.72 (2H, d, 8 Hz)	116.2	6.73 (d, 2H, 8.4 Hz)	116.5	6.74 (2H, dd, 2.4 Hz)	116.24	6.71 (d, 2H, 8.4 Hz)
4'	C	157.05		156.9		157.1		156.86	
7'	CH_2	35.91	2.75 (2H, t, 7 Hz)	35.8	2.76 (t, 2H, 7.5 Hz)	36.0	2.77 (2H, t, 7.2 Hz)	35.88	2.74 (2H, t, 6.9 Hz)
8'	CH_2	42.66	3.47 (2H, t, 7 Hz)	42.5	3.47 (t, 2H, 7.5 Hz)	42.7	3.48 (2H, t, 7.2 Hz)	42.54	3.46 (2H, t, 6.9 Hz)
	OCH_3	56.45	3.87 (3H, s)	56.4	3.85 (3H, s)	56.6	3.89 (3H, s)	56.33	3.87 (3H, s)

group was present, as evidenced by absorption at 1588 cm^{-1} and between 880 and 680 cm^{-1} . It was also identified that in this isolate, the aliphatic functional group (CH_2) at 3010 cm^{-1} , carbonyl ($\text{C}=\text{O}$) at 1700 cm^{-1} , and ester at 1210 cm^{-1} .

The results of the antibacterial test of pure isolates versus crude extracts and active fractions, as illustrated in Fig. 7, indicate that the isolates are promising against the biofilm bacterium *P. aeruginosa*. The antibacterial activity was relatively high against *P. aeruginosa*, with a minimum inhibitory concen-

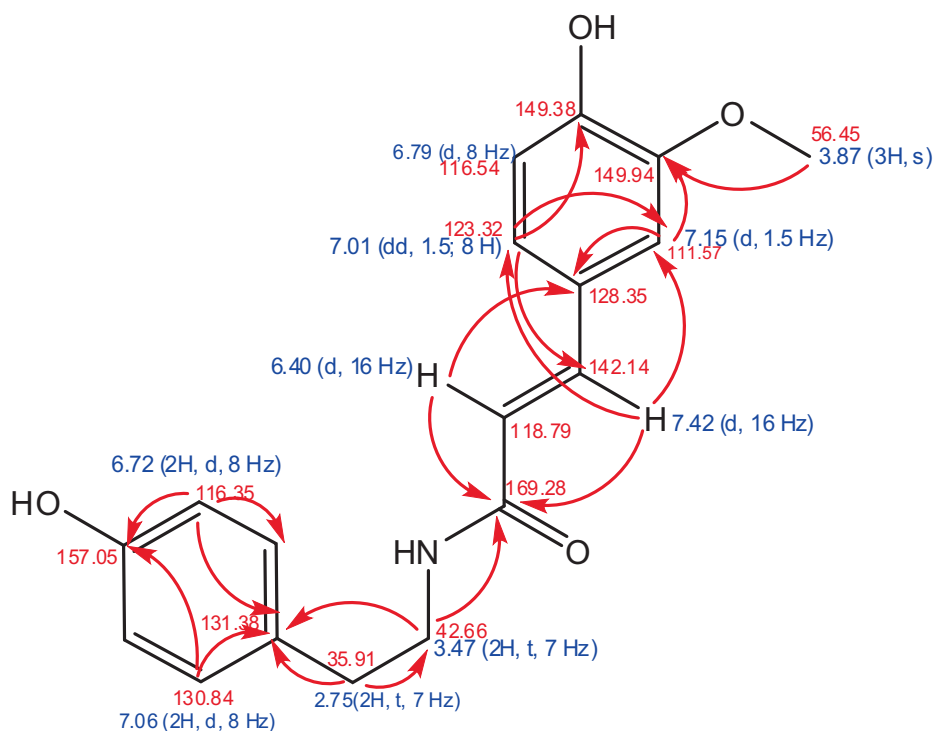


Fig. 5 Chemical shift value and summary HMBC correlation for an isolate from *T. cordifolia*.

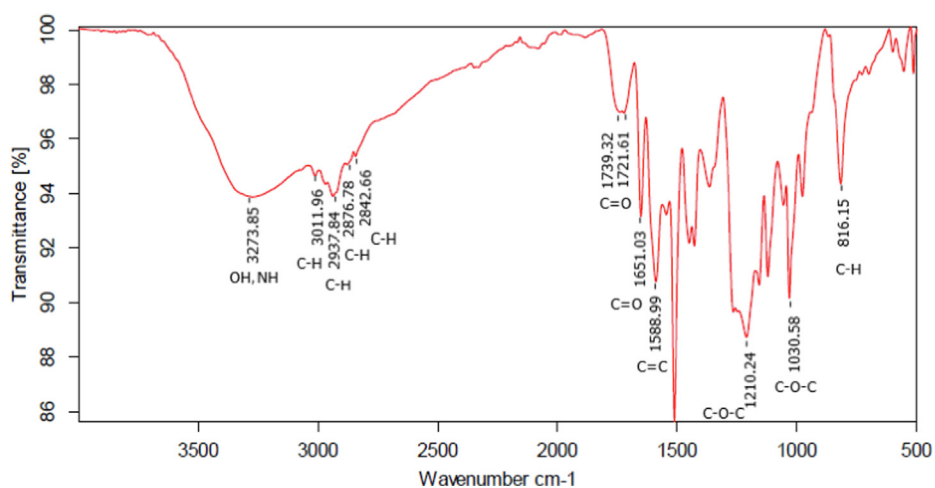


Fig. 6 FT-IR spectra of isolate results from *T. cordifolia*.

tration of 32 $\mu\text{g/mL}$, as demonstrated by the bacterial test data. Furthermore, the MIC results in Fig. 7 support the relationship between phenolic and flavonoid content and antibacterial activity. The antibacterial activity increases with increasing concentrations of TPC and TFC in the active fraction of the crude extract (Table 3).

Several studies have shown that moupinamide or N-trans feruloyltyramine (NTF) compounds isolated from plants show various bioactivities, such as *Liriope muscari* (Liliaceae), which exhibits antioxidant activity (Li et al., 2012), and *Celtis africana*, which possesses anti-inflammatory and

antioxidant activity (Al-Taweel et al., 2012). Other studies have discovered that N-trans feruloyltyramine from the fruit of *Lycium barbarum* can potentially be a neuroprotective and neurogenic agent for age-related brain diseases (Khan et al., 2021). *Sidastrum paniculatum* was effective against *Aedes aegypti* L (Marques et al., 2022). *Piper walllichii* has been shown to exhibit antibacterial pathogenic activity (Nongmai et al., 2022). Based on the data and some literature, it appears that moupinamide is responsible for the antibacterial activity of the plant extracts and isolates investigated in this study.

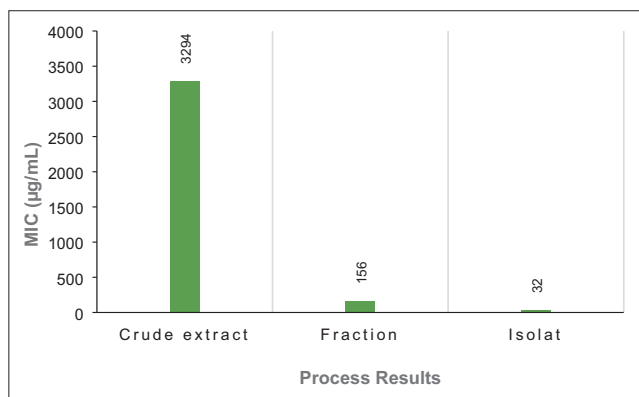


Fig. 7 Comparison of MIC values for crude extracts, active fractions, and isolates from *T. cordifolia* plants.

4. Conclusions

Bioactive compounds were successfully isolated from *T. cordifolia* stems through extraction, fractionation, and isolation. The minimum inhibitory concentration (MIC) values were 3294, 156, and 32 µg/mL for the crude extract, active fraction, and isolate of *T. cordifolia*, respectively. The total phenol active fraction was 38.44 mg GAE/g, while the total flavonoid content was 79.46 mg QE/g. The isolated bioactive compound confirmed by NMR and FT-IR spectroscopy is *N-trans*-feruloyltyramine or moupinamide, with a molecular ion weight of 314 M/Z (M + H)⁺. Compounds isolated from this plant exhibit significant antimicrobial activity. The isolated compound moupinamide could be responsible for the high antibacterial activity against *P. aeruginosa* bacteria. Our findings indicate that the bioactive isolate from *T. cordifolia* is a great potential source of green material with the prospect of inhibiting the biofilm of *P. aeruginosa*, which is responsible for microbial corrosion. Before using this component as a green antimicrobial biocide, the anti-biocorrosion performance on metals must be evaluated.

Author contributions

A.R. proposed and conceptualized the research, designed, and performed experiments, analysed the data, and drafted, reviewed, and final-edited the manuscript. M.H. interpreted the NMR data and reviewed and edited the manuscript. P. D.N.L. extracted and isolated the bioactive compounds. M. E.P. assessed antibacterial activity. C.V. advised, reviewed, and edited the manuscript. A.M. supervised, advised, and reviewed the manuscript. A.A. advised and reviewed the manuscript. All authors have read, reviewed, and approved the manuscript.

6. Data supporting

The original contributions made in the study have been included in both the article and [supplementary material](#). Any queries concerning the information that has been decoded can be directed to the corresponding author.

Acknowledgements

This work was supported by the University of Indonesia through the “Hibah Publikasi Terindeks Internasional (PUTI

2022” programs under contract number NKB-1451/UN2.RST/HKP.05.00/2022. The authors also appreciate the National Research and Innovation Agency (BRIN) for its support of laboratory facilities.

Appendix A. Supplementary material

Supplementary data to this article can be found online at <https://doi.org/10.1016/j.arabjc.2023.105014>.

References

- Ahmad, W., Jantan, I., Bukhari, S.N.A., 2016. *Tinospora Crispa* (L.) Hook. f. & Thomson: a review of its ethnobotanical, phytochemical, and pharmacological aspects. *Front. Pharmacol.* 7 (59), 1–19. <https://doi.org/10.3389/fphar.2016.00059>.
- Al-Taweel, A.M., Perveen, S., El-Shafae, A.M., Fawzy, G.A., Malik, A., Afza, N., Iqbal, L., Latif, M., 2012. Bioactive phenolic amides from *Celtis Africana*. *Molecules* 17 (3), 2675–2682. <https://doi.org/10.3390/molecules17032675>.
- Amaro, C.A., Botello, M.-C., Herrera-Ruiz, M., Román-Ramos, R., Aguilar-Santamaría, L., Tortoriello, J., Jiménez-Ferrer, E., 2014. Hypoglycemic and hypotensive activity of a root extract of *Smilax Aristolochiifolia*, Standardized on *N-Trans-Feruloyl-Tyramine*. *Molecules* 19 (8), 11366–11384. <https://doi.org/10.3390/molecules190811366>.
- Chang, C.C., Yang, M.H., Wen, H.M., Chern, J.C., 2002. Estimation of total flavonoid content in propolis by two complementary colorimetric methods. *J. Food Drug Anal.* 10 (3), 178–182. <https://doi.org/10.38212/2224-6614.2748>.
- Elboughdiri, N., 2018. Effect of time, solvent-solid ratio, ethanol concentration and temperature on extraction yield of phenolic compounds from olive leaves. *Eng. Technol. Appl. Sci. Res.* 8 (2), 2805–2808. <https://doi.org/10.48084/etasr.1983>.
- Ida Madiha, Y., Rukayadi, Y., Norhayati, H., 2017. Effects of extraction conditions on yield, total phenolic contents and antibacterial activity of Methanolic *Cinnamomum Zeylanicum* Blume leaves extract. *Int. Food Res. J.* 24 (2), 779–786.
- Jia, R.u., Yang, D., Dake, X.u., Tingyue, G.u., 2017. Anaerobic Corrosion of 304 stainless steel caused by the pseudomonas aeruginosa biofilm. *Front. Microbiol.* 8 (2335), 1–9. <https://doi.org/10.3389/fmicb.2017.02335>.
- Jiang, Y., Lingling, Y.u., Wang, M.H., 2015. *N-Trans-Feruloyltyramine* Inhibits LPS-Induced NO and PGE2 Production in RAW 264.7 Macrophages: involvement of AP-1 and MAP Kinase Signalling Pathways. *Chem. Biol. Interact.* 235, 56–62. <https://doi.org/10.1016/j.cbi.2015.03.029>.
- Kadir, D.H., 2021. Statistical evaluation of main extraction parameters in twenty plant extracts for obtaining their optimum total phenolic content and its relation to antioxidant and antibacterial activities. *Food Sci. Nutr.* 9 (7), 3491–4349. <https://doi.org/10.1002/fsn3.2288>.
- Khan, Z., Hong, S.M., Lee, J.W., Moon, E.Y., Huh, J., Chang, K.A., Kim, S.Y., 2021. Potential of *N-Trans Feruloyl Tyramine* from *Lycium Barbarum* Fruit Extract on Neurogenesis and Neurotrophins; Targeting TrkA/ERK/CREB Signaling Pathway. *J. Funct. Foods* 80 (104432), 1–9. <https://doi.org/10.1016/j.jff.2021.104432>.
- Lekbach, Y., Dake, X.u., El Abed, S., Dong, Y., Dan Liu, M., Khan, S., Koraiichi, S.I., Yang, K.e., 2018. Mitigation of microbiologically influenced corrosion of 304L stainless steel in the presence of pseudomonas aeruginosa by *Cistus Ladanifer* leaves extract. *Int. Biodeter. Biodegr.* 133, 159–169. <https://doi.org/10.1016/j.ibiod.2018.07.003>.
- Li, W.J., Cheng, X.L., Liu, J., Lin, R.C., Wang, G.L., Shu Shan, D.u., Liu, Z.L., 2012. Phenolic compounds and antioxidant activities of

- Liriope Muscari. *Molecules* 17 (2), 1797–1808. <https://doi.org/10.3390/molecules17021797>.
- Marciales, A., Peralta, Y., Haile, T., Crosby, T., Wolodko, J., 2019. Mechanistic microbiologically influenced corrosion modeling—A review. *Corros. Sci.* 146, 99–111. <https://doi.org/10.1016/j.corsci.2018.10.004>.
- Marques, S.D.G., Fernandes, D.A., Teles, Y.C.F., Menezes, R.P.B., Maia, M.S., Scotti, M.T., Agra, M.F., Silva, T.M.S., de Fátima, M., de Souza, V., 2022. *Sidastrum Paniculatum* (L.) Fryxell (Malvaceae): A Promising Source of Bioactive Sulfated Flavonoids Against *Aedes Aegypti* L. *Front. Pharmacol.* 12 (760156), 1–13. <https://doi.org/10.3389/fphar.2021.760156>.
- Nawaz, H., Shad, M.A., Rehman, N., Andaleeb, H., Ullah, N., 2020. Effect of solvent polarity on extraction yield and antioxidant properties of phytochemicals from bean (*Phaseolus Vulgaris*) seeds. *Braz. J. Pharm. Sci.* 56 (e17129), 1–9. <https://doi.org/10.1590/s2175-97902019000417129>.
- Nikitasari, A., Sundjono, G.P., Royani, A., 2020. Polyphosphate performance for inhibiting corrosion of heat exchanger materials. *Int. J. Corrosion Scale Inhibition* 9 (2), 745–756. <https://doi.org/10.17675/2305-6894-2020-9-2-22>.
- Nongmai, C., Kanokmedhakul, K., Promgool, T., Paluka, J., Suwanphakdee, C., Kanokmedhakul, S., 2022. Chemical constituents and antibacterial activity from the stems and leaves of *Piper Wallichii*. *J. Asian Nat. Prod. Res.* 24 (4), 344–352. <https://doi.org/10.1080/10286020.2021.1933959>.
- Othman, A., Amen, Y., Matsumoto, M., Nagata, M., Shimizu, K., 2021. Bassiamide A, a New Alkaloid from Xero-Halophyte *Bassia Indica* Wight. *Nat. Prod. Res.* 36 (14), 3610–4368. <https://doi.org/10.1080/14786419.2021.182572>.
- Parthipan, P., Elumalai, P., Narenkumar, J., Machuca, L.L., Murugan, K., Karthikeyan, O.P., Rajasekar, A., 2018. *Allium Sativum* (Garlic Extract) as a green corrosion inhibitor with biocidal properties for the control of MIC in carbon steel and stainless steel in oilfield environments. *Int. Biodeter. Biodegr.* 132, 66–73. <https://doi.org/10.1016/j.ibiod.2018.05.005>.
- Parthipan, P., Cheng, L., Rajasekar, A., 2021. *Glycyrrhiza Glabra* extract as an eco-friendly inhibitor for microbiologically influenced corrosion of API 5LX carbon steel in oil well produced water environments. *J. Mol. Liq.* 333. <https://doi.org/10.1016/j.molliq.2021.115952>.
- Pirrung, S.M., Parruca da Cruz, D., Hanke, A.T., Berends, C., Van Beckhoven, R.F., Eppink, M.H., Ottens, M., 2018. Chromatographic parameter determination for complex biological feedstocks. *Biotechnol. Prog.* 34 (4), 1006–1018. <https://doi.org/10.1002/btpr.2642>.
- Priyanto, J.A., Prastya, M.E., Sinarawadi, G.S., Datu'salamah, W., Avelina, T.Y., Yanuar, A.I.A., Azizah, E., Tachrim, Z.P., Mozef, T., 2022. The antibacterial and antibiofilm potential of *Paederia Foetida* Linn. leaves extract. *J. Appl. Pharm. Sci.* 12 (10), 117–124. <https://doi.org/10.7324/JAPS.2022.121012>.
- Pu, Y., Dou, W., Tingyue, G.u., Tang, S., Han, X., Chen, S., 2020. Microbiologically influenced corrosion of Cu by nitrate reducing marine bacterium *Pseudomonas Aeruginosa*. *J. Mater. Sci. Technol.* 47, 10–19. <https://doi.org/10.1016/j.jmst.2020.02.008>.
- Ramesh, J., Amanpreet, K., Tapan, M.K., Priya, B., 2016. Phytochemical analysis and biological studies of Indian medicinal plants *Myristica Fragrans* and *Tinospora Cordifolia*. *Int. J. Adv. Res.* 4 (5), 245–258. <https://doi.org/10.21474/IJAR01>.
- Ravisankar, P., Anusha, S., Supriya, K., Ajith Kumar, U., 2019. Fundamental chromatographic parameters. *Int. J. Pharm. Sci. Rev. Res.* 55 (2 (9)), 46–50.
- Royani, A., Hanafi, M., Manaf, A., 2022. Prospect of plant extracts as eco-friendly biocides for microbiologically influenced corrosion: a review. *Int. J. Corrosion Scale Inhibition* 11 (3), 862–888. <https://doi.org/10.17675/2305-6894-2022-11-3-1>.
- Royani, A., Hanafi, M., Julistiono, H., Dinoto, A., Lotulung, P.D., Manaf, A., 2023. The potential of *Tinospora Cordifolia* extracts as antibacterial material against *pseudomonas Aeruginosa*. *Trends Sci.* 20 (1), 1–13. <https://doi.org/10.48048/tis.2023.3884>.
- Satheesh, S., Ba-Akdah, M.A., Al-Sofyani, A.A., 2016. Natural antifouling compound production by microbes associated with marine macroorganisms — A review. *Electron. J. Biotechnol.* 21, 26–35. <https://doi.org/10.1016/j.ejbt.2016.02.002>.
- Serrano Cardona, S.L., Muñoz Mata, E., 2013. *Paraninfo Digital*. *Early Hum. Dev.* 83 (1), 1–11. <https://doi.org/10.1016/j.earlhumdev.2006.05.022>.
- Singh, D., Chaudhuri, P.K., 2017. Chemistry and Pharmacology of *Tinospora Cordifolia*. *Nat. Prod. Commun.* 12 (2), 299–308. <https://doi.org/10.1177/1934578x1701200240>.
- Singleton, V.L., Orthofer, R., Lamuela-Raventós, R.M., 1999. Analysis of total phenols and other oxidation substrates and antioxidants by means of Folin-Ciocalteu reagent. *Methods Enzymol.* 299, 152–178. [https://doi.org/10.1016/S0076-6879\(99\)99017-1](https://doi.org/10.1016/S0076-6879(99)99017-1).
- Soi-ampornkul, R., Myint, E.E.P., Thangnipon, W., Tantarungsee, N., Mitrpant, C., Tuchinda, P., Nobsathian, S., Vatanashevvanopakorn, C., 2022. N-Trans-Feruloyltyramine Protects Human Neuroblastoma SK-N-SH Cell Line Against H₂O₂-Induced Cytotoxicity. *Nat. Prod. Commun.* 17 (8), 1–8. <https://doi.org/10.1177/1934578X221117312>.
- Sukiman, M., Irawan, C., Ismail, I.D., Putri, A.U., Dewanta, A., Septian, W.A., 2022. Optimization of ultrasound-assisted extraction of *Tinospora Crispa* Stem, phytochemical screening, total phenolic content and anti gout potential activity. *Pharmacognosy J.* 14 (2), 308–314. <https://doi.org/10.5530/pj.2022.14.39>.
- Sun, G., Strebl, M., Merz, M., Blamberg, R., Huang, F.-C., McGraphery, K., Hoffmann, T., Schwab, W., 2019. Glucosylation of the Phytoalexin N-feruloyl Tyramine modulates the levels of pathogen-responsive metabolites in *Nicotiana Benthamiana*. *Plant J.* 100, 20–37. <https://doi.org/10.1111/tpj.14420>.
- Swaroop, B.S., Victoria, S.N., Manivannan, R., 2016. *Azadirachta Indica* leaves extract as inhibitor for microbial corrosion of copper by *Arthrobacter Sulfureus* in neutral PH conditions—a remedy to blue green water problem. *J. Taiwan Inst. Chem. Eng.* 64, 269–278. <https://doi.org/10.1016/j.jtice.2016.04.007>.
- Tran, T.T., Dang, H.P., Nguyen, T.N., 2019. Chemical constituents from methanolic extract of *Solanum Procumbens* Lour (Solanaceae). *Vietnam J. Sci. Techno. Eng.* 61 (3), 9–11. [https://doi.org/10.31276/vjste.61\(3\).09-11](https://doi.org/10.31276/vjste.61(3).09-11).
- Verma, C., Ebenso, E.E., Bahadur, I., Quraishi, M.A., 2018. An overview on plant extracts as environmental sustainable and green corrosion inhibitors for metals and alloys in aggressive corrosive media. *J. Mol. Liq.* 266, 577–590. <https://doi.org/10.1016/j.molliq.2018.06.110>.
- Vongsak, B., Sithisarn, P., Mangmool, S., Thongpraditchote, S., Wongkrajang, Y., Gritsanapan, W., 2013. Maximizing Total Phenolics, total flavonoids contents and antioxidant activity of *Moringa Oleifera* Leaf extract by the appropriate extraction method. *Ind. Crop. Prod.* 44, 566–571. <https://doi.org/10.1016/j.indcrop.2012.09.021>.
- Widyawati, S., Pains, T.D., Budianta, W., Kusuma, F.A., Wijaya, E. L., 2014. Difference of solvent polarity to phytochemical content and antioxidant activity of *Pluchea Indicia less* leaves extracts. *Int. J. Pharmacognosy Phytochem. Res.* 6 (4), 850–885.
- Xu, S., Liu, Y., Xiang, L., Zhou, F., Li, H., Yongjian, S.u., Xinyi, X. u., Wang, Q.i., 2018. Metabolites Identification of Bioactive Compounds *Daturaturin A*, *Daturametelin I*, *N-Trans-Feruloyltyramine*, and *Cannabisin F* from the Seeds of *Datura Metel* in Rats. *Front. Pharmacol.* 9 (731), 1–9. <https://doi.org/10.3389/fphar.2018.00731>.
- Yusoff, M., Hamid, H., Houghton, P., 2014. Anticholinesterase inhibitory activity of quaternary alkaloids from *Tinospora Crispa*. *Molecules* 19 (1), 1201–1211. <https://doi.org/10.3390/molecules19011201>.